Desalination and Water Treatment
www.deswater.com

doi:10.5004/dwt.2018.21423

106 (2018) 21–31
February

High selectivity polyamide reverse osmosis membrane enhanced by aminosilane-modified silicalite-1 nanozeolites

Hai Huang, Huifeng Zhang, Yangyang Wei, Man Zhao, Yushan Zhang*

The Institute of Seawater Desalination and Multipurpose Utilization, State Oceanic Administration, Tianjin 300192, China, Tel. +86-022-87898130, email: Huanghaiisdmu@163.com (H. Huang), Tel. +86-022-87898130, email: hfzhang@126.com (H. Zhang), Tel. +86-022-87898130, email: weiyangy@126.com (Y. Wei), Tel. +86-022-87898130, email: zhaomancrystal@163.com (M. Zhao), Tel. +86-022-87898159, email: yushanzhang@hotmail.com (Y. Zhang)

Received 1 May 2017; Accepted 7 September 2017

ABSTRACT

Nanozeolites are proved to improve water permeability when they are incorporated into polyamide reverse osmosis membranes. But this incorporation also brings selectivity loss due to the non-selective defects derived from poor affinity of nanozeolites to polyamide matrix and aggregation of these nanoparticles. This work developed surface aminosilane modification involving anchoring 3-aminopropyltriethoxysilane onto nanosized silicalite-1 before integration with polyamide matrix *via* interfacial polymerization. Results of fourier transform infrared spectroscopy and X-ray photo electron spectroscopy showed that modified silicalite-1 particles formed a stronger covalent interaction with polyamide matrix than pristine ones, implying a better compatibility between these two materials. Characterization with dynamic lights cattering and transmission electron microscope manifested that modified nanozeolites formed much smaller nano-clusters both in preparing solution and resulting membrane than pristine ones, suggesting that aggregation was mitigated. Performance evaluation showed that the membrane incorporated with aminosilanized silicalite-1 zeolites (an optimum integrating concentration (0.05%, *w/v*)) exhibited superior NaCl rejection (98.6%) to that with pristine silicalite-1 (Rejection = 97.1%). A 67% increase in water flux (58.5 L/m^2·h) over the bare PA membrane was also achieved by applying the modified nanozeolites. The strategy of aminosilane-modification in this work is proved potential to prevent rejection loss for nanozeolites-enhanced RO membranes.

Keywords: Thin film composite membrane; Silicalite-1 nanozeolites; Aminosilane modification; Defects elimination; High selectivity

1. Introduction

Global water and energy scarcity have driven many attempts to develop reverse osmosis (RO) technology for desalination due to its higher efficiency and lower expense compared with thermal based distillation method. The thin film composite (TFC) membranes, fabricated through smart interfacial polymerization, have been widely applied in current RO process. This kind of membranes consists of top ultra thin polyamide (PA) layers delivering separative property and porous substrates, e.g. polysulfone ultrafiltration membranes, which provide the essential mechanical strength. As the PA layers are extremely dense and greatly decreased in thickness, TFC membranes have distinct advantages in the permeability and selectivity over previous asymmetric cellulose acetate membranes [1]. To obtain higher permeability, TFC membranes have been recently enhanced by integrating PA layers with many porous nano-materials (*e.g.* zeolites [2], silica [3] and metal organic frameworks [4]) by virtue of their porous structures as additional pathways for water transport [5,6]. Among above nano-materials, nanozeolites are most preferred in membrane enhancement due to their excellent stability and regularity of frameworks.

Until now, a variety of nanozeolites,including the types of LTA [7–9], MFI [10] and FAU [11,12] (abbreviation of the

*Corresponding author.

inventors) with different tunnel structures, have been investigated for the nanozeolites-PA membrane fabrication. Several common features of this membrane species have been already observed. Firstly, most studies demonstrate that nanozeolites' integration can be realized *via* a facile nanozeolites-dispersion in reactive phases before membrane polymerization. So this integration seems commercially superior to complicated conventional methods such as regulations of polymeric monomers [13], modification of membrane surface [13] as well as invasive post-treatments [14]. Secondly, recent studies have revealed that alkane reactive phase is more suitable to act as the dispersion medium than aqueous phase [15,16]. That results from the fact that PA polymerization is primarily processing in alkane phase, so nanozeolites will rationally be more completely integrated with PA matrix though alkane phase dispersion [17,18]. Besides, the nanozeolites-reinforcement is always exciting with a commonly over-50% increase in water flux, implying the potential application of nanozeolites in RO membranes [10–12].

In spite of these attractive advantages, increasing incorporation of nanozeolites makes it more difficult to keep membrane with an acceptable selectivity [10,12,19]. This problem primarily stems from two factors [15]. The first one is the weak interaction between nanozeolites and PA matrix which is hard to receive a seamless integration. This incompatibility caused interface defects between the two materials [20,21]. The second one is the over-strong interaction within nanoparticles which leads to undesirable aggregation and following formation of nano-clusters when nanozeolites are dispersed into alkane phase for membrane preparation. The senano-clusters are inclined to grow up, resulting in larger microvoids and eventually bringing non-selective defects to membranes [22].

Both incompatibility and aggregation problems are commonly observed in most of other nanoparticles-enhanced membranes/films [21,23,24]. To mitigate incompatibility, surface activation to these nanoparticles is widely performed as an effective strategy [25,26]. This surface modification generally offers nanozeolites with functional groups which are easy to covalently bond with polymer matrix. By this means, an intensified covalent interaction is introduced between these two materials for compatibility improvement. Particularly in the preparation of PA membranes, the alkane reactive-phase will certainly contain acyl chloride monomers. So nanozeolites are expected to be linked with resulting PA matrix via pre-reacting with acyl chlorides during dispersion period. In fact, nanozeolites have been observed to form ester linkage with acyl chlorine as a result of their surficialsilanol groups (-Si-OH) [15]. However, the pH sensitivity and propensity to hydrolysis of ester linkage make it unreliable in long-term RO operation. Therefore, surface activation is still necessary to form another chemical linkage with better stability. As to aggregation, a simple ultrasonic-assisted pre-treatment is previously proposed to make nanozeolites well-dispersed in preparing solution for membrane [20,24]. However during the interfacial polymerization of nanozeolites-PA RO membrane, hydrophilic nanozeolites are scattered into extremely hydrophobic (alkane) reactive-phase, so they have a strong propensity of aggregation which needs further enhancement for dispersibility. Recent investigations also conducted surface modification on nanozeolites to regulate their surface polarity. By improving the surface affinity to solvent molecules, nanozeolites' mutual aggregation can be obviously suppressed [20,21,23,27–29].

Since surface modification is promising to improve both compatibility and dispersibility, it may be feasible to develop a synchronous modification to settle both of the two issues simultaneously. It is obviously more convenient compared with applying individual methods to solve the two issues, respectively. However, this synchronous strategy is rarely proposed in previous researches of nanozeolites-PA membranes because of the incomplete understanding on these two factors resulting in selectivity loss.

As a synchronous modification, we reported an aminosilane coupling agent to modify silicalite-1 nanozeolites' surface for simultaneous amination and silanization. Here, silicalite-1 was used because it had been proven as an ideal candidate to offer the TFC RO membrane with higher water permeability and better stability [10]. As is expected, the amination can enable nanozeolites to pre-react with acid chloride monomers in alkane phase and then, form amide linkage with resulting PA matrix, which is more stable than original ester linkage. Meanwhile, silanization is supposed to suppress the nanozeolites aggregation *via* introducing nonpolar hydrophobic-elements with desirable affinity to alkane solvent. Both of the nanozeolites and resulting membranes were comprehensively characterized for their physicochemical properties. Also, a comparative evaluation of membrane performance was conducted in case of pristine and modified nanozeolites.

2. Experimental

2.1. Materials

Fumed silica powder (0.2 μm–0.3 μm in average particle size, Aldrich), Tetra-*n*-propylammonium hydroxide (TPAOH, ~40%, Aldrich) and sodium hydroxide (NaOH, ≥98%, Aldrich) were utilized for silicalite-1 synthesis. Poly(vinyl alcohol) (PVA-1799, Suzhou Chemical Industry Co. Ltd) was used to assist template agent removal during sintering. For surface modification on silicalite-1 particles, 3-aminopropyltriethoxysilane (APTES, 98%, Aldrich) and *n*-heptane (99%, Fuchen Co. Ltd, Tianjin, China) were used as purchased. For membrane fabrication, porous polysulfone membranes (Pureach Tech. Ltd, Beijing, China) were applied as substrate. Trimesoyl chloride (TMC, 98%, Aldrich) and *m*-phenyldiamine (MPD, >99%, Aldrich), sodium chloride and *n*-hexane were purchased from Sinopharm Chemical Reagent Co. Ltd. Deionized (DI) water generated by a Milli-Q ultrapure water purification system was applied to prepare all solutions for subsequent experiments.

2.2. Synthesis of silicalite-1 nanozeolites

Silicalite-1 nanozeolites were synthesized with hydrothermal method [30]. The synthesis solution was prepared at room temperature by mixing TPAOH (25 mL), NaOH (0.35 g) and DI water (0.2 mL) under stirring until a clear solution is achieved. This precursor solution was heated

to 80°C and then fumed silica powder (5.0 g) was added stepwise under vigorous stirring until solution turned back clear. It was left undisturbed to cool down to room temperature for about 3 h. Afterwards, this solution was transferred to an PTFE lined autoclave and subjected to hydrothermal reaction for 13 h under 80°C in a convective oven. The resultant silicalite-1 nanozeolites were collected by cycles of centrifugation (10000 rpm, 6 min) and rinse with DI-water until pH of supernatant came to 7.

Calcination was applied to remove template molecule strapped in the nanozeolites' pores during synthesis [10]. Typically, silicalite-1 colloid was added into PVA aqueous solution (2%, w/v) under violent stirring for 40–60 min as a pre-treatment for better dispersion. Ultrasonication was then conducted to this mixture for 10–20 min for complete dispersion. This composite was then poured onto a Teflon dish in order to form silicalite-1/PVA thin films after drying in an oven (80°C) for 5 h. Finally, the product of well-defined nanozeolites was obtained after a calcination of these composite films at 550°C for 12 h (heating and cooling rate of 1°C min^{-1}). The obtained silicalite-1 nanozeolites were dried under vacuum at 100°C and caped in a tightly sealed bottle and then kept in a desiccator for later use.

2.3. Surface modification of silicalite-1 nanozeolites

APTES was employed to modifysilicalite-1 nanozeolites' surface for silanization and amination [20,21]. APTES (3 mL) and synthesized nanozeolites (1 g) were mixed in *n*-heptane (100 mL) under violent stirring for 24 h. Then centrifugation and rinse were applied to the product within 200 mL of *n*-heptane and 300 mL of methanol for purification. Finally, the modified nanozeolites were dried under vacuum overnight at room temperature followed by additional 3 h at elevated temperature (200°C) to thoroughly remove residual solvent.

2.4. Preparation of nanozeolites-PA membranes

A typical inter facial polymerization procedure was adopted to prepare PA RO membrane [31]: PS substrate was contacted with aqueous solution of MPD (2%, *w/v*) for about 5 min. Then residual aqueous solution on substrate surface was squeezed off by a stainless steel roller. Subsequently, the substrate was treated with alkane (*n*-hexane) solution of TMC (0.1%, *w/v*) for 40 s. Then the resulting PA membrane underwent heat treatment at 100°C for 5 min and following water rinse. In a similar procedure, the nanozeolites-incorporated membrane was prepared by scattering these nanoparticles into the alkane phase. Ultra sonication was applied to the nanozeolites solution for about 1 h with temperature controlled at 25°C for a better dispersion. In this paper, pristine (unmodified) and modified nanozeolites integrated membranes were denoted as O-PA and M-PA, respectively. As control, the bare membrane sample without any nanozeolites was labelled as B-PA.

2.5. Characterization of silicalite-1 nanozeolites

X-ray power diffraction patterns (XRD; D8 Advance, BRUKER AXS, Germany) of X'pert diffractometer using Cu Kα radiation were applied to determine the crystalline feature. Scanning electron microscopy (SEM; JSM-5610LV, JEOL, Japan) was applied to detect surface morphology. Mean size of the nanoparticles was estimated by manually measuring the SEM images. Fourier transform infrared spectroscopy (FTIR; Thermo Fisher, IS50, USA) and X-ray photoelectron spectroscopy (XPS, K-alpha,Thermo Fisher, USA) were employed to analysis the surface chemistry of nanozeolites. Particularly, FTIR spectra were taken with a resolution of 4 cm^{-1} and 128 accumulating scans. XPS spectra were taken by a Kratos Axis Ultra DLD (Shimadzu-KRATOS, Japan) Infinity Spectrometer with a spinning speed of around 4.0 kHz using RF fields of 32 kHz. The dispersibility of nanozeolites in alkane solution was estimated *via* dynamic lights cattering (DLS, Zetasizer Nano ZSP, Malvern Instrument, UK) to determine their nano-clusters' size. This measurement were carried out using dilute alkane solution containing synthesized pristine nanozeolites and modified products both at a loading concentration of 0.05% (w/v). An ultrasonic treatment was conducted in advance for approximately 1 h at 25°C just like the membrane preparation process.

2.6. Characterization of membranes

Surface morphologies of fabricated membranes were imaged by SEM. Besides, transmission electron microscope (TEM; Hitachi-H7650, Japan) was used to estimate the distribution of nanozeolites in resulting PA top layers. For this purpose, membrane samples were peeled off from the nonwoven and treated with chloroform to remove polysulfone substrate. A contact angle goniometer (CA; Digidrop, GBX, France) was used to evaluate the membrane wettability. For accuracy, every sample was tested from five different sites, which was ultimately estimated with the average.

A lab-scale cross-flow test device was used to estimate the RO performance of membranes. NaCl aqueous solution (2000 ppm) at 25°C was applied as bulk feed solution and effective membrane area was 15.9 cm^2. Membrane samples were subject to a pressure of 1.55 MPa for 1 h ahead of performance evaluation. NaCl content in permeate and bulk feed solution were both measured in terms of conductivity meter. The water flux and NaCl rejection were calculated using Eqns. (1) and (2):

$$J = \frac{V}{S \times \Delta t} \tag{1}$$

$$R = \frac{C_f - C_p}{C_f} * 100\% \tag{2}$$

where V is the volume of permeate during the operation time Δt, S is the effective area, C_p and C_f are the NaCl concentration in the permeate and bulk feed solution, respectively.

The estimate the intrinsic transport property of membranes, water permeability $A\ (= J/\Delta P)$ was calculated from the water flux (J) for the specified applied pressure (ΔP). Salt (NaCl) permeability coefficient $B\ (= J(1–R)/R)$ was accordingly determined from the flux (J) and solute rejection (R) [32].

3. Results and discussion

3.1. Characterization of APTES-modification on nanozeolites

3.1.1. Crystalline and morphology characterization

XRD patterns of the pristine and modified nanozeolites presented in Fig. 1 validated the synthesized particles as silicalite-1 phase and further estimated the effect of modification on crystalline structure. Characteristic high peaks can be observed at 2θ = 7.94°, 8.90°, 23.2°, 23.8° and 45° in both samples, which are typical features in silicalite-1 zeolites [33]. This result not only confirms the success synthesis of silicalite-1, but also implies that APTES-modification does not alter nanozeolites' crystalline structure as reported in other studies [21,29]. Moreover, the intact crystalline structure is significant to nanozeolites-PA membrane because it is essential to introduce proper channels.

SEM detection was used to measure the sizes of synthesized nanozeolites and evaluate the influence of modification on nanoparticles' morphology. Given that the average thickness of PA layer ranges from 100 to 200 nm, nanozeolites are often expected to be about 100 nm in diameter to ensure a complete incorporation in PA polymer matrix [7, 19,32]. In this work, nanozeolites were readily fine-tuned through subtle regulation of hydrothermal synthesis condition. As exhibited in Fig. 2a, ideal nanozeolites with the size of about 130 n min diameter were prepared. Additionally, Fig. 2b manifests that APTES-modified nanozeolites display the similar morphology (*i.e.* size and geometry) to pristine sample, suggesting that APTES-modification will not change the surface feature of nanozeolites.

3.1.2. Surface chemical characterization

Fig. 3 depicts the reactions supposed to occur on nanozeolites' surface during the whole nanozeolites-PA membrane fabrication. The first step is APTES modification when the hydrophilic silicon hydroxyl (Si-OH) is replaced by hydrophobic siloxane fragment. The influence of APTES modification on nanozeolites' surface chemistry was determined by FTIR. As shown in Fig. 4a, both the pristine and modified nanozeolites have intensive adsorption bands at 1113 and 800 cm^{-1}. These two peaks are typical for zeolites that are attributed to the asymmetric and symmetric stretching vibration of Si-O-Si bond, respectively [21]. Meanwhile, modified nanozeolites have several emerging peaks at 2933, 2856 and 1467 cm^{-1}, of which the first two bands are assigned to aliphatic C-H group stretching [34] and the last one is caused by C-H bending [35]. These C-H groups are obviously introduced by APTES fragment. Furthermore, a characteristic peak at 1565 cm^{-1} is observed in modified nanozeolites, which is corresponding to the N-H bending of the terminal a mine of APTES [34]. All above results prove the success of APTES modification of silicalite-1.

3.2. Compatibility evaluation

It has been well demonstrated that APTES-modified nanozeolites' surfaces are remarkably amine-terminated. Hence, they are expected to form amide bonds with TMC monomers containing acyl chlorides for better compatibility with resulting PA matrix. To validate this amidation reaction, modified nanozeolites were also surface-analysed after they had undergone an ultrasonic treatment in the alkane solution containing TMC. This case is denoted as

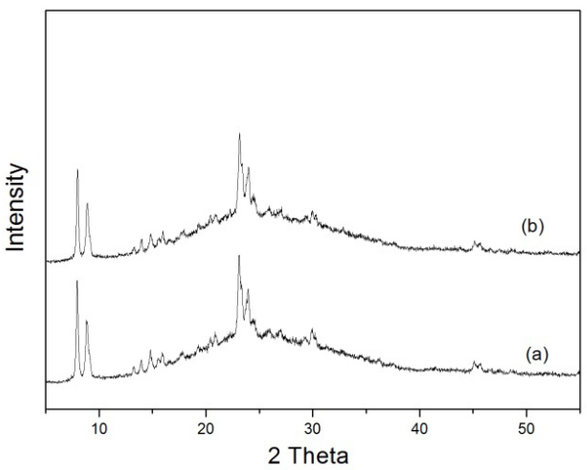

Fig. 1. Powder XRD patterns of (a) pristine and (b) APTES-modified silicalite-1 nanozeolites.

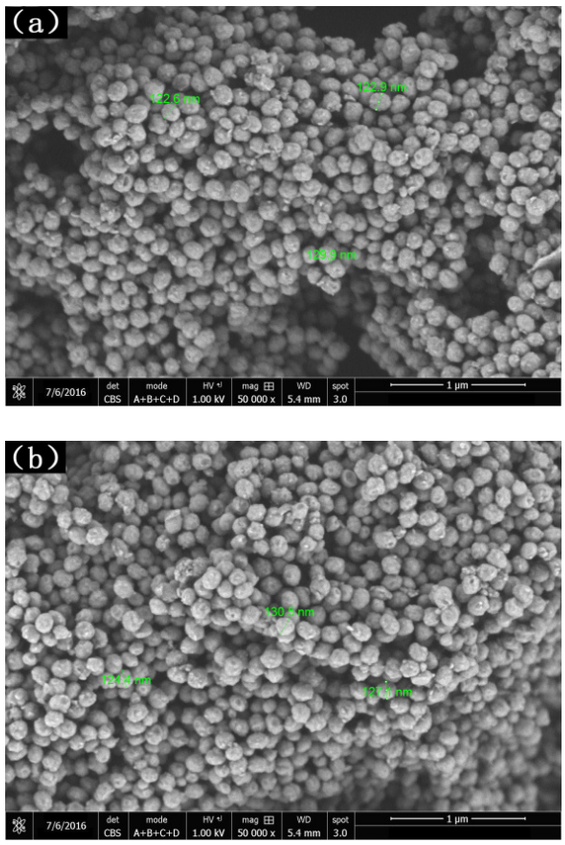

Fig. 2. SEM images of pristine (a) and APTES-modified (b) silicalite-1 nanozeolites.

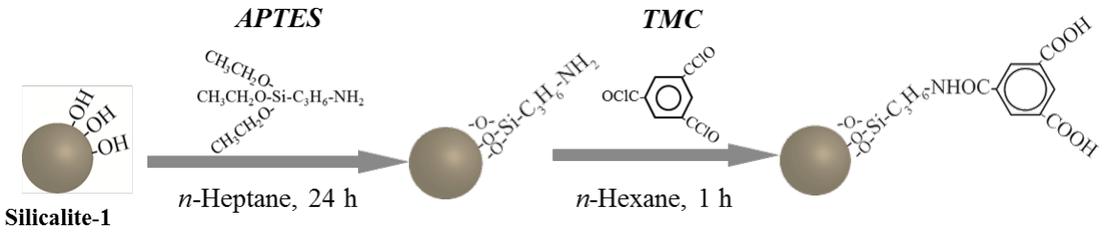

Fig. 3. Schematic of APTES modification and following TMC reaction happened to silicalite-1.

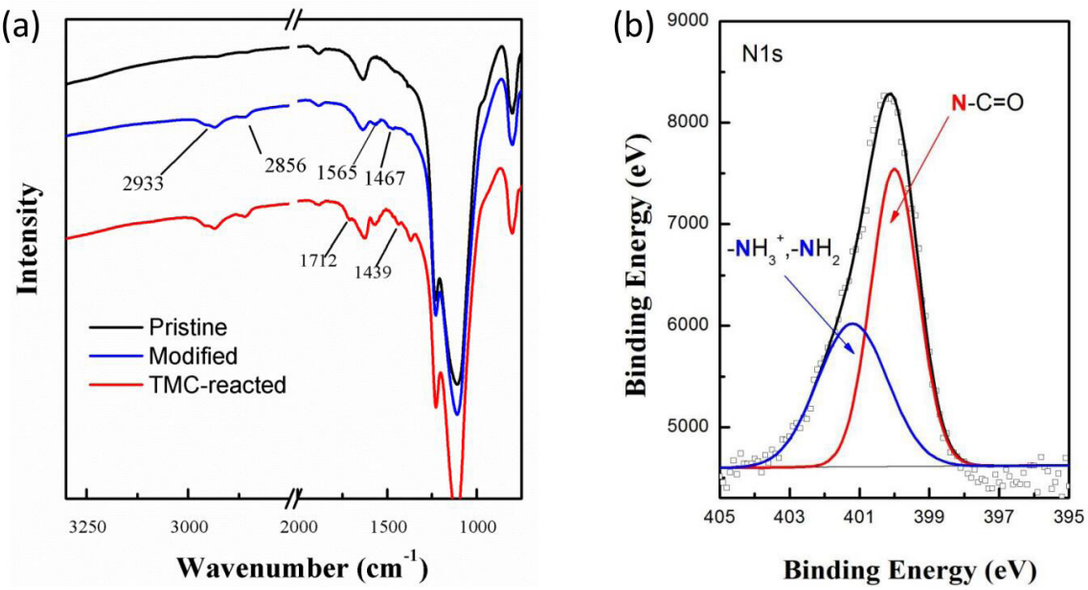

Fig. 4(a). FTIR spectra of pristine, APTES-modified and TMC-reacted nanozeolites. (b) XPS analysis of N-element of APTES-modified nanozeolites after reacted with TMC.

'TMC-reacted' in Fig. 4a, a new peak at 1712 cm^{-1} is ascribed to C=O stretching of TMC [36] and another peak at 1439 cm^{-1} is assigned to the symmetric stretching vibrations of the carboxylic group after the hydrolysis of TMC's acyl chlorides (Fig. 3) [37]. This result is similar to the case of pristine nanozeolites containing only hydroxyl groups, which is explained by esterification with TMC [15]. Therefore, it can be analogously inferred that amidation indeed proceeds between amine-terminated nanozeolites and TMC as illustrated by Fig. 3. Furthermore, XPS survey (probing depth < 10 nm) was also applied to analyse the N-element on the surface of TMC-reacted nanozeolites. Given that amidation changes the chemical state of N-element from amine ($–NH_2$ and $–NH_3^+$) to amide (–COHN–), a quantitative analysis should be performed to estimate the amidation extent *via* resolving the characteristic N 1 s peak in XPS spectrum. As indicated by Fig. 4b, this N 1 s peak actually consists of two split peaks with binding energy of 400 and 401.2 eV, which are assigned to amide and amine nitrogen, respectively [38]. Then the ratio of amide to amine nitrogen of nanozeolites can be calculated by integration of corresponding peak areas, which eventually equals to about 1.4:1. That is to say, a 58.3% of amines from APTES modification have been consumed to form amide bonds with TMC monomers during the dispersion pre-treatment. Hence, silicalite-1 nanozeolites after APTES modification are promising to chemically couple with PA matrix *via* stable amide bonds, which is significant to improve the compatibility and thus, eliminate the interface defects. It is necessary to note that protonated ($–NH_3^+$) and deprotonated ($–NH_2$) amine-N forms are not be decomposed because their peaks are too close in XPS.

3.3. Dispersibility evaluation

3.3.1. DLS analysis

DLS analysis was used for evaluating the dispersibility of nanozeolites in alkane solution. As demonstrated in Fig. 5a, there exist nano-clusters with size around 1000 nm in solution of pristine nanozeolites, which are obviously larger than average nanozeolites size (≈130 nm) shown in SEM charaterization. That suggests a severe aggregation occurring as illustrated in Fig. 5c. As to APTES-modified nanozeolites, by contrast, Fig. 5b indicates that these nano-clusters narrow to about 240 nm. That means APTES modification is able to remarkably suppress the aggregating phenomenon, which is attributed to the solvent affinity brought by silanization as illustrated by Fig. 5d.

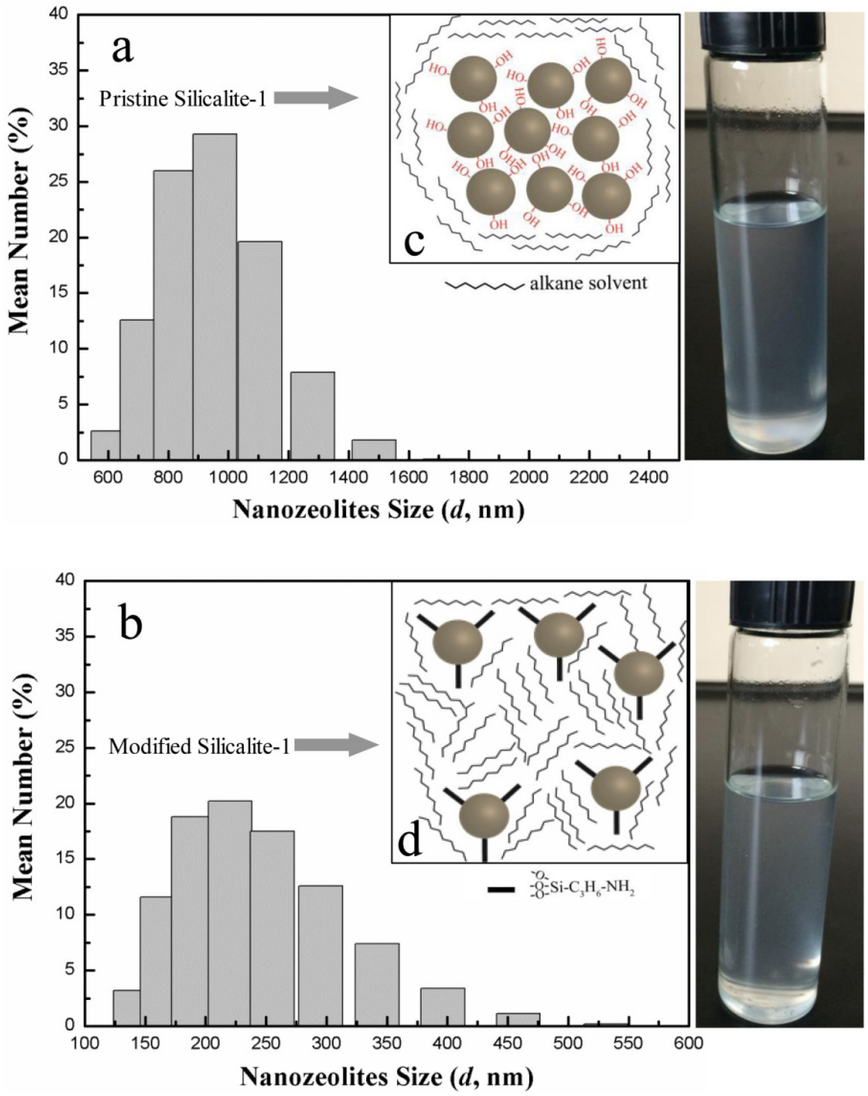

Fig. 5. Particle diameter distribution charaterization of DLS in alkane phase.

3.3.2. TEM analysis

Nanozeolites dispersibility in reactive phase is expected to affect their ultimate distribution in resulting membrane. To investigate this distribution, PA selective layers integrated with pristine and APTES-modified nanozeolites (0.05%, *w/v*) were both imaged by TEM. As illustrated in Fig. 6, pristine nanozeolites (see Fig. 6a) are likely to aggregate and even form observed nano-clusters in PA membrane, possibly resulting from their poor dispersibility in alkane phase as demonstrated in Fig. 5a. Fortunately, this undesirable tendency is supressed in the modified case (see Fig. 6b) with less and smaller nano-clusters in PA matrix. Given this fact, APTES-modification is definitely helpful to promote the distribution homogeneity of nanozeolites, which has already been proved beneficial to membrane selectivity since the non-selective voids can be effectively prevented [24,27,39].

3.4. Characterization of nanozeolites in corporation on membrane

3.4.1. Surface wettability

Fig. 7 shows the effect of the nanozeolites incorporation on the surface wettability of resulting membranes. In the beginning, both O-PA and M-PA experience a similar gradual decrease in contact angle from the original B-PA of 65° to about 45° with more nanozeolites loading. This variation may result from an increased interfacial free-energy given by nanoparticles since they have high specific area. That means more active surface-atoms (with affinity to water) are introduced into membrane [40,41]. This hydrophilic tendency is always observed in other cases of nano-materials mixed membranes involving other nanozeolites [11,32], carbon nanotube [42] and graphene oxide [43]. Moreover, M-PA is relatively hydrophobic compared with O-PA since APTES

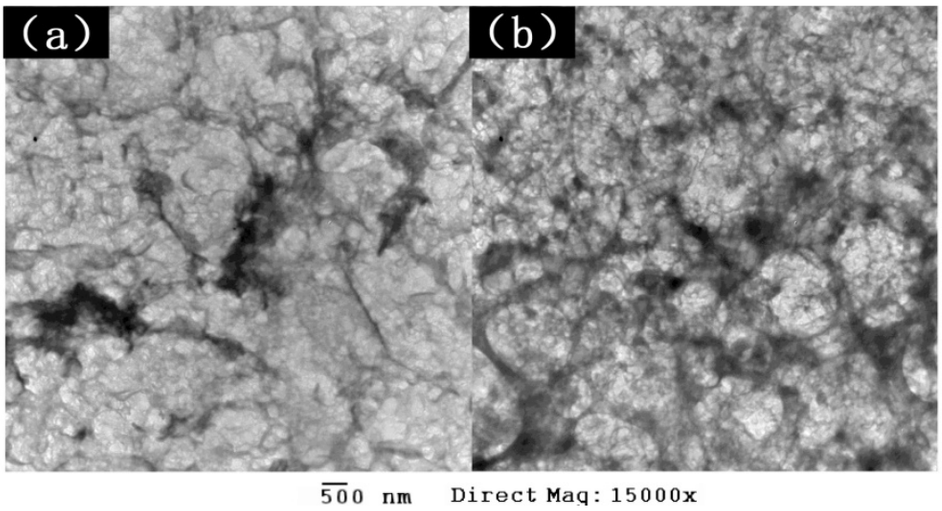

Fig. 6. TEM images of nanozeolites incorporated (0.05%, *w/v*) PA membranes with (a) pristine and (b) APTES-modified silicalite-1 nanozeolites.

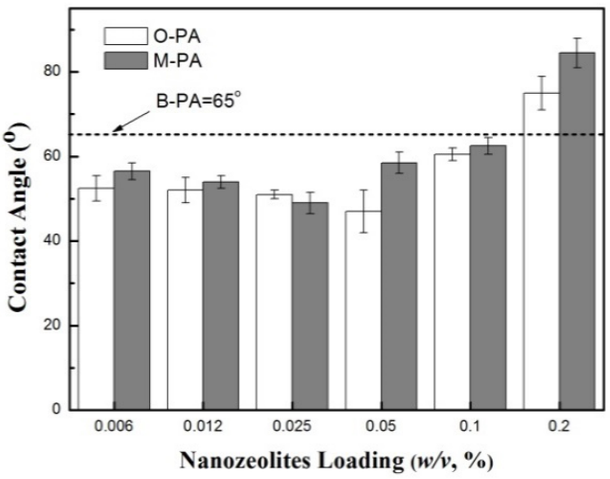

Fig. 7. Contact angle of membranes with pristine (O-PA) and APTES modified (M-PA) nanozeolites.

modification will bring hydrophobic siloxane fragment to nanozeolites. It is also notable that an excessive incorporation will instead make the membrane hydrophobic, which may be rationally ascribed to the incomplete polymerization of PA layer in result of excessive nanozeolites used.

3.4.2. Morphology characterization

Fig. 8 presents SEM images of the surface morphology of PA membranes incorporated with pristine and APTES-modified nanozeolites. Initially, both O-PA and M-PA membranes are observed with typical 'peak-valley' feature like B-PA samples within a moderate loading concentration of nanozeolites [7]. Just like the changes shown from Figs. 8a to 8d as well as 8e–8h, an increased nanozeolites loading comes to make these 'peak' zones become larger on the selective PA layer. This phenomenon is also reported in previous studies of nanozeolites-PA membranes [11,32], which is commonly ascribed to the extended reaction zone for interfacial polymerization just like the cases employing co-solvents [44,45]. To be specific, nanozeolites, initially dispersed in alkane phase, might conduct hydration between their surface hydroxyl groups and water molecules at the interface of aqueous-alkane phases. Then much heat will be released and thus, make aqueous and alkane solutions miscible [46,47]. This interpretation can also account for the fact that O-PA's 'peak-vally' feature appears more obvious than M-PA (especially seen in Fig. 8c and 8d), since APTES modification have partly consumed the hydroxyl groups of nanozeolites and then suppress the miscible effect. Generally, these developed 'peak' zones probably decrease the density of PA layers and then promote water-permeation. Figs. 8e–h indicate that an excessive nanozeolites loading over 0.1% adversely interpret the formation of a dense PA selective layer that is essential to high selectivity. For example, both O-PA and M-PA membranes have transformed from initially dense to porous morphology at the 0.1% loading (see Figs. 8e and 8f), which becomes more obvious at 0.2% loading displayed by Figs. 8g and 8h. All above results suggest that there exists an optimal loading concentration to regulate the membrane structure for a desirable separation performance.

3.4.3. Membrane performance

The variation of membrane permeability and selectivity are shown in Fig. 9 to study the impacts of nanozeolites integration and following APTES-modification on separation performance. As to membrane selectivity (see Fig. 9a), NaCl rejection of O-PA obviously decreased with increasing nanozeolites loading compared with the bare PA membrane of 99%, which is commonly supposed to result from the defects inside the aggregated nano-clusters or/as well

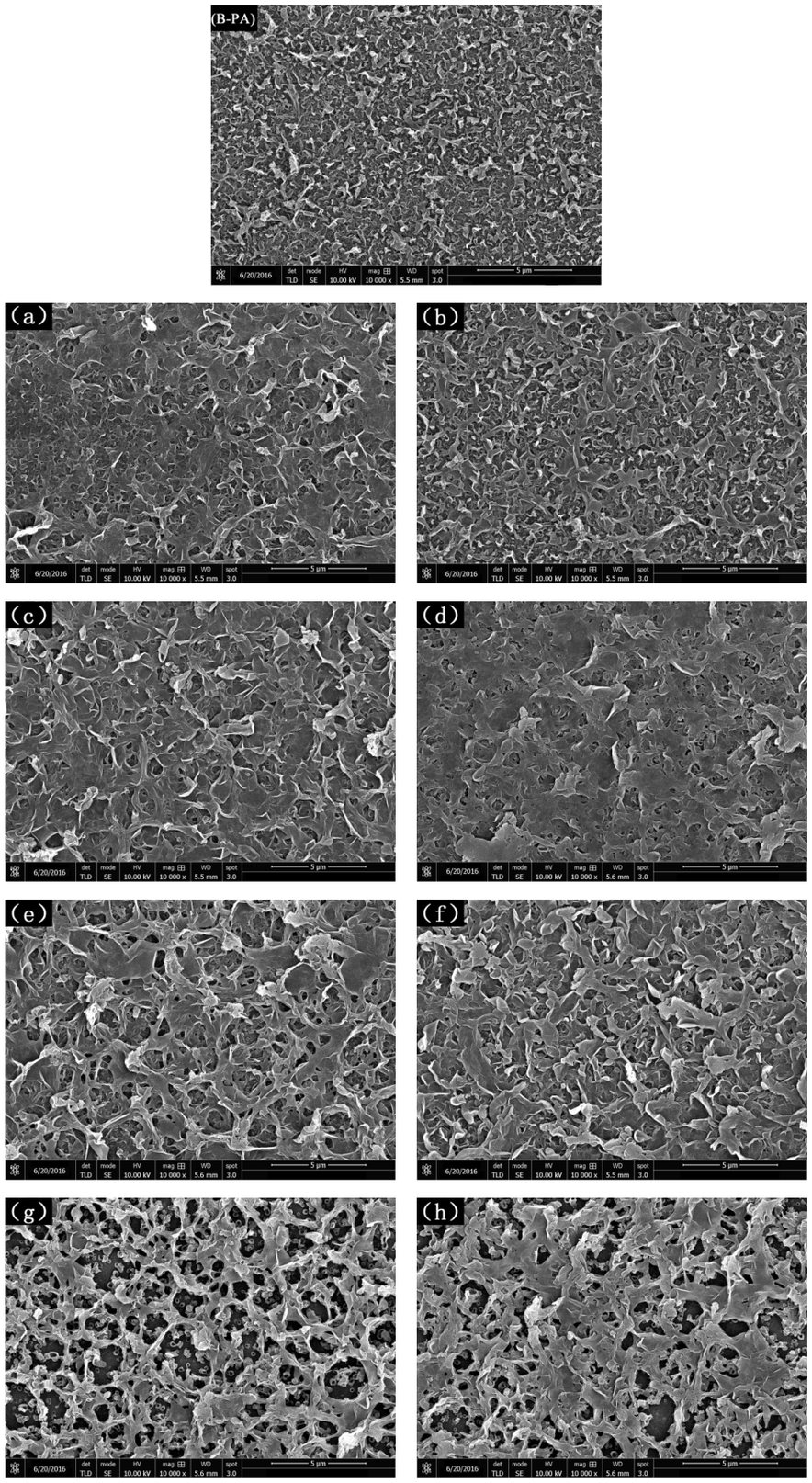

Fig. 8. SEM surface morphology of B-PA, O-PA with (a) 0.025%, (c) 0.05%, (e) 0.1%, (g) 0.2% loading and M-PA with (b) 0.025%, (d) 0.05%, (f) 0.1%, (h) 0.2% loading.

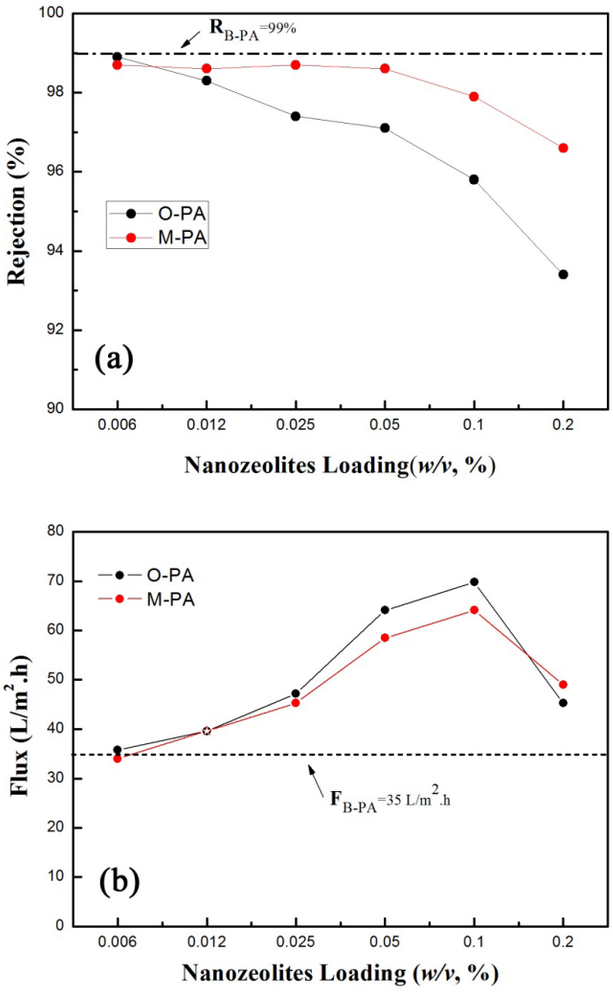

Fig. 9. RO performance of O-PA and M-PA in different loading concentration of nanozeolites in alkane phase: (a) rejection and (b) flux.

as on the interface between PA and nanozeolites [15,24,27]. Fortunately, M-PA succeeds to maintain a preferably stable rejection of 98.6% until 0.05% of nanozeolites concentration when O-PA decreases to 97.1%. That means selectivity deterioration could be remarkably mitigated after the incorporated nanozeolites experienced APTES-modification as showed in Fig. 3. Considering above factors on dispersibility (proved by DLS and TEM) and compatibility (proved by FTIR and XPS) improvements, APTES-modification has been proved as a necessary regulation of nanozeolites to help maintain a high selectivity by repressing the nanozeolites aggregation as well as promote the compatibility of PA matrix and nanozeolites. This conclusion has also been supported in other nano-material enhancing membrane processes such as pervaporation and gas separation [27,39,48].

Fig. 9b exhibits the effect of nanozeolites loading on membrane flux. As a matter of fact that more 'water channels' are introduced into PA membrane, both O-PA and M-PA would experience an evident flux increase from the bare PA membrane of 35 L/m^{2}h. However, M-PA inevitably

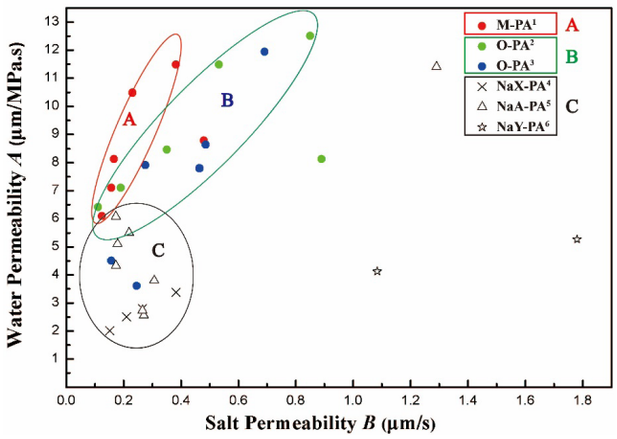

Fig. 10. Performance comparison of different nanozeolites-PA RO membranes. (Data from: 1,2: present work; 3:[10]; 4:[11]; 5:[7,15,32]; 6:[19];).

remains to be uncompetitive with O-PA in flux since most of M-PA's defects have been eliminated by APTES modification. In spite of this fact, the permeability improvement of 67% to initial B-PA (at 0.05% loading) is still remarkable in the case of M-PA. What's more important, M-PA's flux enhancement is hardly accompanied with selectivity loss unlike the case of O-PA. In addition, excessive nanozeolites seem to have side-effect on both selectivity and permeability, which may be ascribed to the incomplete formation of PA layer interrupted by nanozeolites.

Most of typical nanozeolites-PA membranes have been summarized in Fig. 10 in terms of their membrane performances in order to evaluate the effectiveness of our modifying strategy. Here, all the membranes are classified into three groups to facilitate comparison. As Fig. 10 shows, Zone A represents the M-PA membranes with APTES-modified silicalite-1 in present work; Zone B indicates the O-PA membranes incorporated with pristine silicalite-1 in both present and previous work [10]; Zone C includes the cases with other types of nanozeolites. Although some membranes of Zone B are worse than membranes of Zone C on the aspect of salt permeability, most of membranes in both Zone A and Zone B are considerably better than membranes of Zone C on the aspect of water permeability. This result manifests the advantages of silicalite-1 as the membrane reinforcer over other types of nanozeolites used. What's more, Zone A is superior to Zone B with a lower increase in salt permeability when water permeability is enhanced. Fig. 10 suggests that APTES-modification is significant for satisfactory membrane selectivity.

4. Conclusion

Silicalite-1 nanozeolites modified with APTES have been proved to maintain satisfactory selectivity when they are integrated with PA RO membranes. By introducing siloxane fragment, this aminosilane modification is found to make the nanozeolites well-dispersed in reactive phase and then homogenously distributed in resulting membranes. More-

over, XPS analysis of N-element discovers that aminosilane modification develops firm bonds between silicalite-1 and PA matrix through amidation reaction. Those two facts are just expected to eliminate the membrane defects both inside the aggregated nano-clusters and on the nanozeolites-PA interface, respectively. Just as the following RO assessment showed, the membrane enhanced by modified silicalite-1 had a preferable selectivity to the membrane employing pristine silicalite-1 within an appropriate loading concentration. In summary,this paper demonstrates that aminosilane modification is a promising nanozeolites regulation for better separation performance especially on the respect of high selectivity. Considering that membrane defects are commonly present in other nano-material enhanced membranes, this modification strategy may be also instructive in a larger application.

Acknowledgments

This work was supported by the National Key Research and Development Program of China (2017YFC0403901), Central Research and Public Service Institutes of Basic Research Program of China(2016-T10 and 2016-T11).

References

[1] A.F. Ismail, M. Padaki, N. Hilal, T. Matsuura, W.J. Lau, Thin film composite membrane - Recent development and future potential, Desalination, 356 (2015) 140–148.
[2] W.J. Lau, S. Gray, T. Matsuura, D. Emadzadeh, J.P. Chen, A.F. Ismail, A review on polyamide thin film nanocomposite (TFN) membranes: History, applications, challenges and approaches, Water Res., 80 (2015) 306–324.
[3] M. Bao, G. Zhu, L. Wang, M. Wang, C. Gao, Preparation of monodispersed spherical mesoporous nanosilica-polyamide thin film composite reverse osmosis membranes via interfacial polymerization, Desalination, 309 (2013) 261–266.
[4] J. Duan, Y. Pan, F. Pacheco, E. Litwiller, Z. Lai, I. Pinnau, High-performance polyamide thin-film-nanocomposite reverse osmosis membranes containing hydrophobic zeolitic imidazolate framework-8, J. Membr. Sci., 476 (2015) 303–310.
[5] M.U. Ari, M.G. Ahunbay, M. Yurtsever, A. Erdem Senatalar, Molecular dynamics simulation of water diffusion in MFI-type zeolites, J. Phys. Chem. B, 113 (2009) 8073–8079.
[6] L. Li, J. Dong, T.M. Nenoff, Transport of water and alkali metal ions through MFI zeolite membranes during reverse osmosis, Separ. Purif. Technol., 53 (2007) 42–48.
[7] B.H. Jeong, E.M.V. Hoek, Y.S. Yan, A. Subramani, X.F. Huang, G. Hurwitz, A.K. Ghosh, A. Jawor, Interfacial polymerization of thin film nanocomposites: A new concept for reverse osmosis membranes, J. Membr. Sci., 294 (2007) 1–7.
[8] M.L. Lind, B.H. Jeong, A. Subramani, X. Huang, E.M.V. Hoek, Effect of mobile cation on zeolite-polyamide thin film nanocomposite membranes, J. Mater. Res., 24 (2009) 1624–1631.
[9] M.L. Lind, D. Eumine Suk, T.V. Nguyen, E.M.V. Hoek, Tailoring the structure of thin film nanocomposite membranes to achieve seawater RO membrane performance, Environ. Sci. Technol., (2010) 8230–8235.
[10] H. Huang, X. Qu, X. Ji, X. Gao, L. Zhang, H. Chen, L. Hou, Acid and multivalent ion resistance of thin film nanocomposite RO membranes loaded with silicalite-1 nanozeolites, J. Mater. Chem. A, 1 (2013) 11343–11349.
[11] M. Fathizadeh, A. Aroujalian, A. Raisi, Effect of added NaX nano-zeolite into polyamide as a top thin layer of membrane on water flux and salt rejection in a reverse osmosis process, J. Membr. Sci., 375 (2011) 88–95.
[12] H. Dong, L. Zhao, L. Zhang, H.L. Chen, C.J. Gao, W.S.W. Ho, High-flux reverse osmosis membranes incorporated with NaY zeolite nanoparticles for brackish water desalination, J. Membr. Sci., 476 (2015) 373–383.
[13] W. Li, L. Lou, Y. Hai, C. Fu, J. Zhang, Polyamide thin film composite membrane using mixed amines of thiourea and m-phenylenediamine, RSC Adv., 5 (2015) 54125–54132.
[14] H.D. Raval, J.J. Trivedi, S.V. Joshi, C.V. Demurari, Flux enhancement of thin film composite RO membrane by controlled chlorine treatment, Desalination, 250 (2010) 945–949.
[15] H. Huang, X. Qu, H. Dong, L. Zhang, H. Chen, Role of NaA zeolites in the interfacial polymerization process towards a polyamide nanocomposite reverse osmosis membrane, RSC Adv., 3 (2013) 8203–8207.
[16] G.S. Lai, W.J. Lau, S.R. Gray, T. Matsuura, R.J. Gohari, M.N. Subramanian, S.O. Lai, C.S. Ong, A.F. Ismail, D. Emazadah, M. Ghanbari, A practical approach to synthesize polyamide thin film nanocomposite (TFN) membranes with improved separation properties for water/wastewater treatment, J. Mater. Chem. A, 4 (2016) 4134–4144.
[17] V. Freger, Kinetics of film formation by interfacial polycondensation, Langmuir, 21 (2005) 1884–1894.
[18] F. Yuan, Z. Wang, X. Yu, Z. Wei, S. Li, J. Wang, S. Wang, Visualization of the formation of interfacially polymerized film by an optical contact angle measuring device, J. Phys. Chem. C, 116 (2012) 11496–11506.
[19] N. Ma, J. Wei, R. Liao, C.Y. Tang, Zeolite-polyamide thin film nanocomposite membranes: Towards enhanced performance for forward osmosis, J. Membr. Sci., 405 (2012) 149–157.
[20] N. Wang, J. Liu, J. Li, J. Gao, S. Ji, J.R. Li, Tuning properties of silicalite-1 for enhanced ethanol/water pervaporation separation in its PDMS hybrid membrane, Micropor. Mesopor. Mater., 201 (2015) 35–42.
[21] X. Zhuang, X. Chen, Y. Su, J. Luo, S. Feng, H. Zhou, Y. Wan, Surface modification of silicalite-1 with alkoxysilanes to improve the performance of PDMS/silicalite-1 pervaporation membranes: Preparation, characterization and modeling, J. Membr. Sci., 499 (2016) 386–395.
[22] S.Y. Lee, H.J. Kim, R. Patel, S.J. Im, J.H. Kim, B.R. Min, Silver nanoparticles immobilized on thin film composite polyamide membrane: characterization, nanofiltration, antifouling properties, Polym. Adv. Technol., 18 (2007) 562–568.
[23] M. Biçen, N. Kayaman Apohan, S. Karataş, F. Dumludağ, A. Güngör, The effect of surface modification of zeolite 4A on the physical and electrical properties of copolyimide hybrid films, Micropor. Mesopor. Mater., 218 (2015) 79–87.
[24] X.Y. Qu, H. Dong, Z.J. Zhou, L. Zhang, H.L. Chen, Pervaporation separation of xylene isomers by hybrid membranes of PAAS filled with silane-modified zeolite, Ind. Eng. Chem. Res., 49 (2010) 7504–7514.
[25] H. Zhao, S. Qiu, L. Wu, L. Zhang, H. Chen, C. Gao, Improving the performance of polyamide reverse osmosis membrane by incorporation of modified multi-walled carbon nanotubes, J. Membr. Sci., 450 (2014) 249–256.
[26] H. Wu, B. Tang, P. Wu, Optimizing polyamide thin film composite membrane covalently bonded with modified mesoporous silica nanoparticles, J. Membr. Sci., 428 (2013) 341–348.
[27] P. Wei, X. Qu, H. Dong, L. Zhang, H. Chen, C. Gao, Silane-modified NaA zeolite/PAAS hybrid pervaporation membranes for the dehydration of ethanol, J. Appl. Polym. Sci., 128 (2013) 3390–3397.
[28] S.G. Kim, D.H. Hyeon, J.H. Chun, B.H. Chun, S.H. Kim, Nanocomposite poly(arylene ether sulfone) reverse osmosis membrane containing functional zeolite nanoparticles for seawater desalination, J. Membr. Sci., 443 (2013) 10–18.
[29] H. Zhou, Y. Su, X. Chen, S. Yi, Y. Wan, Modification of silicalite-1 by vinyltrimethoxysilane (VTMS) and preparation of silicalite-1 filled polydimethylsiloxane (PDMS) hybrid pervaporation membranes, Separ. Purif. Technol., 75 (2010) 286–294.
[30] J. Yu, Chapter 3 - Synthesis of Zeolites, in: H.v.B.A.C. Jiří Čejka, S. Ferdi (Eds.) Studies in Surface Science and Catalysis, Elsevier, 2007, pp. 39–103.

[31] M. Mulder, Preparation of Synthetic Membranes, in: Basic Principles of Membrane Technology, Springer Netherlands, Dordrecht, 1996, pp. 71–156.
[32] M.L. Lind, A.K. Ghosh, A. Jawor, X.F. Huang, W. Hou, Y. Yang, E.M.V. Hoek, Influence of zeolite crystal size on zeolite-polyamide thin film nanocomposite membranes, Langmuir, 25 (2009) 10139–10145.
[33] X.J. Zhuang, X.R. Chen, Y. Su, J.Q. Luo, W.F. Cao, Y.H. Wan, Improved performance of PDMS/silicalite-1 pervaporation membranes via designing new silicalite-1 particles, J. Membr. Sci., 493 (2015) 37–45.
[34] N. Majoul, S. Aouida, B. Bessais, Progress of porous silicon APTES-functionalization by FTIR investigations, Appl. Surf. Sci., 331 (2015) 388–391.
[35] P. Larkin, Chapter 6 - IR and Raman spectra-structure correlations: characteristic group frequencies, in: Infrared and Raman Spectroscopy, Elsevier, Oxford, 2011, pp. 73–115.
[36] E. Igbinigun, Y. Fennell, R. Malaisamy, K.L. Jones, V. Morris, Graphene oxide functionalized polyethersulfone membrane to reduce organic fouling, J. Membr. Sci., 514 (2016) 518–526.
[37] Z.G. Chen, H.L. Chen, H. Hu, M.X. Yu, F.Y. Li, Q. Zhang, Z.G. Zhou, T. Yi, C.H. Huang, Versatile synthesis strategy for carboxylic acid-functionalized upconverting nanophosphors as biological labels, J. Amer. Chem. Soc., 130 (2008) 3023–3029.
[38] D. Van Thanh, C.Y. Tang, M. Reinhard, J.O. Leckie, Degradation of polyamide nanofiltration and reverse osmosis membranes by hypochlorite, Environ. Sci. Technol., 46 (2012) 852–859.
[39] A.E. Amooghin, M. Omidkhah, A. Kargari, The effects of aminosilane grafting on NaY zeolite-Matrimid (R) 5218 mixed matrix membranes for CO_2/CH_4 separation, J. Membr. Sci., 490 (2015) 364–379.
[40] Y. Liao, T.P. Farrell, G.R. Guillen, M. Li, J.A. Temple, X.G. Li, E.M. Hoek, R.B. Kaner, Highly dispersible polypyrrole nanospheres for advanced nanocomposite ultrafiltration membranes, Mater. Horiz., 1 (2014) 58–64.
[41] R. Dingreville, J.M. Qu, M. Cherkaoui, Surface free energy and its effect on the elastic behavior of nano-sized particles, wires and films, J. Mech. Phys. Solids, 53 (2005) 1827–1854.
[42] L. Zhang, G. Shi, S. Qiu, L. Cheng, H. Chen, Preparation of high-flux thin film nanocomposite reverse osmosis membranes by incorporating functionalized multi-walled carbon nanotubes, Desal. Water Treat., 34 (2011) 19–24.
[43] H.R. Chae, J. Lee, C.H. Lee, I.C. Kim, P.K. Park, Graphene oxide-embedded thin-film composite reverse osmosis membrane with high flux, anti-biofouling, and chlorine resistance, J. Membr. Sci., 483 (2015) 128–135.
[44] A. Akbari, S.M.M. Rostami, Development of permeability properties of polyamide thin film composite nanofiltration membrane by using the dimethyl sulfoxide additive, J. Water Reuse Desal., 4 (2014) 174–181.
[45] T. Kamada, T. Ohara, T. Shintani, T. Tsuru, Optimizing the preparation of multi-layered polyamide membrane via the addition of a co-solvent, J. Membr. Sci., 453 (2014) 489–497.
[46] A.K. Ghosh, B.H. Jeong, X. Huang, E.M.V. Hoek, Impacts of reaction and curing conditions on polyamide composite reverse osmosis membrane properties, J. Membr. Sci., 311 (2008) 34–45.
[47] T.A. Ostomel, P.K. Stoimenov, P.A. Holden, H.B. Alam, G.D. Stucky, Host-guest composites for induced hemostasis and therapeutic healing in traumatic injuries, J. Thrombosis Thrombolysis, 22 (2006) 55–67.
[48] H. Sanaeepur, A. Kargari, B. Nasernejad, Aminosilane-functionalization of a nanoporous Y-type zeolite for application in a cellulose acetate based mixed matrix membrane for CO_2 separation, RSC Adv., 4 (2014) 63966–63976.